Author Manuscript

Author Manuscript

Author Manuscript

Author Manuscript

HHS Public Access

Author manuscript

J Control Release. Author manuscript; available in PMC 2024 August 01.

Published in final edited form as:

J Control Release. 2023 August ; 360: 274–284. doi:10.1016/j.jconrel.2023.06.030.

Systemic Administration of Budesonide in Pegylated Liposomes for Improved Efficacy in Chronic Rhinosinusitis

Bhuvanesh Yathavan[a,b], **Alexa Ellis**[c], **Jolanta Jedrzkiewicz**[d], **Nithya Subrahmanyam**[a,b], **Nitish Khurana**[a,b], **Abigail Pulsipher**[a,b,e,*], **Jeremiah Alt**[a,b,e,f,*], **Hamidreza Ghandehari**[a,b,e,f,*]

[a]Department of Molecular Pharmaceutics, University of Utah, Salt Lake City, UT 84112, USA

[b]Utah Center for Nanomedicine, University of Utah, Salt Lake City, UT 84112, USA

[c]College of Pharmacy, University of Utah, Salt Lake City, UT 84112, USA

[d]Department of Pathology, University of Utah, Salt Lake City, UT 84112, USA

[e]Department of Otolaryngology – Head and Neck Surgery, University of Utah School of Medicine, Salt Lake City, Utah, USA

[f]Department of Biomedical Engineering, University of Utah, Salt Lake City, UT 84112, USA

Abstract

Chronic rhinosinusitis (CRS) is a chronic inflammatory condition affecting the nasal and paranasal sinuses of approximately 11.5% of the United States adult population. Oral corticosteroids are effective in controlling sinonasal inflammation in CRS, but the associated adverse effects limit their clinical use. Topical budesonide has demonstrated clinical efficacy in patients with CRS. Herein, we investigated the systemic delivery of liposomes tethered with poly(ethylene glycol) (PEG) and loaded with budesonide in a murine model of CRS. PEGylated liposomes encapsulated with budesonide phosphate (L-BudP) were administered via tail vein injection, and the feasibility of L-BudP to reduce sinonasal inflammation was compared to that of free budesonide phosphate (F-BudP) and topical budesonide phosphate (T-BudP) treatment over a 14-day study period. Compared to a single injection of F-BudP and repeat T-BudP administration, a single injection of L-BudP demonstrated increased and prolonged efficacy, resulting in the significant improvement of sinonasal tissue histopathological scores ($p<0.05$) with decreased immune cell infiltration ($p<0.05$). Toxicities associated with L-BudP and T-BudP treatment, assessed via body and organ weight, as well as peripheral blood liver enzyme and differential white blood cell analyses, were transient and comparable. These data suggest that systemic liposomal budesonide treatment results in improved efficacy over topical treatment.

Keywords

Chronic rhinosinusitis; liposomes; oral glucocorticoids; budesonide; drug delivery

[*]Co-corresponding authors: Hamidreza Ghandehari: hamid.ghandehari@utah.edu; Jeremiah Alt: jeremiah.alt@hsc.utah.edu; Abigail Pulsipher: abigail.pulsipher@utah.edu.

Author Manuscript Author Manuscript Author Manuscript Author Manuscript

1. Introduction

Chronic rhinosinusitis (CRS) is a deteriorating health condition that imposes an immense societal and economic burden and affects up to 11.5% of the adult population in the United States [1]. Beyond sinonasal symptoms, CRS negatively impacts quality of life, causing significant declines in sleep quality, concentration, and daily productivity [2]. Current treatment strategies for CRS heavily rely on topical therapies, such as high-volume saline irrigations and nasal sprays, as well as oral therapies, such as glucocorticoids (GCs) and antibiotics, to reduce symptoms [2, 3]. Some topical treatments, however, have a significant delivery disadvantage, as drug is distributed to the anterior region of the nasal cavity with limited, and variable distribution to the sinus cavities [4, 5]. Moreover, topical treatments experience short residence time due to mucociliary clearance and must overcome physical barriers, such as thick mucus, edema, nasal polyps, and anatomical variations [6], especially in perioperative patients. Budesonide administered via high-volume saline nasal irrigation has demonstrated improved outcomes, but only in post-operative patients with CRS with nasal polyps due to increased access to the sinuses [7]. Oral GCs, are reserved for CRS patients with nasal polyps and have shown to be highly effective in reducing polyp size [2] and underlying sinonasal symptoms [8]. However, the therapeutic effects of oral GCs are short-lived, and their high accumulated doses have been associated with significant side-effects, such as avascular hip necrosis, osteoporosis, adrenal suppression, diabetes, and mood disturbances (*e.g.*, depression, anxiety, and psychosis) [9–11].

In the last two decades, innovations in CRS drug development have focused on local delivery of corticosteroids using nasal delivery devices, such as exhalation devices [12], nebulizers and atomizers [13]. These devices have improved corticosteroid delivery compared to nasal sprays, but require daily administration to maintain clinical efficacy, which reduces patient compliance [6]. Moreover, variations in head position and device usage influence uniform and adequate distribution of the drug to the sinonasal mucosa, limiting efficacy [6, 14, 15]. Recent research has focused on topical controlled release systems with nanoparticles [16] and *in situ* hydrogels [17, 18]. These systems, however, experience limited benefit due to poor penetration across the mucosal layer [6]. The current lack of available effective topical treatments underscores the need for innovative and safe systemic approaches to treating CRS.

The phenomenon of vascular dysregulation has been identified in chronic inflammatory conditions, such as rheumatoid arthritis [19], inflammatory bowel disease [20], and lupus nephritis [21]. This phenomenon has been leveraged to improve steroid accumulation in target tissues, while preventing off-target toxicities through delivery using nanoscale systems. We similarly identified inflammation-driven vascular dysregulation in CRS, characterized by increased angiogenesis, blood vessel morphogenesis, and inter-endothelial gap junction size [22], and demonstrated the size-dependent sinonasal tissue accumulation and retention of liposomes tethered with poly(ethylene glycol) (PEG) for up to 21 days in a murine model of CRS [23]. We therefore hypothesize that corticosteroids delivered with liposomes will lead to enhanced efficacy in reducing sinonasal inflammation, while maintaining low systemic toxicity.

Author Manuscript Author Manuscript Author Manuscript Author Manuscript

In this study, we investigated the safety and efficacy of intravenously administered, budesonide-loaded PEGylated liposomes in a murine model of CRS. Budesonide was selected due to its high potency, short half-life, high protein binding, and safety profile and clinical outcomes when delivered via high-volume saline irrigation in post-operative CRS. Safety was assessed through liver enzyme and differential white blood cell analyses and efficacy through pathological scoring of sinonasal tissue inflammation and immune cell infiltration and compared to normal and CRS controls, as well as animals treated with free and topically administered budesonide.

2. Materials and methods

2.1. Materials

Budesonide phosphate (BudP) was purchased from Symeres (Uitgeest, Netherlands). L-α-phosphatidylcholine, hydrogenated (Soy) (HSPC), 1,2-distearoyl-sn-glycero-3-phosphoethanolamine-N-[methoxy(poly(ethylene glycol))-2000] (DSPE-PEG2000) were obtained from Avanti Polar Lipids (Birmingham, AL, USA). *A. fumigatus* extracts were obtained from Stallergenes-Greer Laboratories (Lenoir, NC, USA). Simulated body fluid (SBF) was obtained from Biochemazone (Leduc, Alberta, Canada). All other chemicals were purchased from Sigma Aldrich (St. Louis, MO, USA).

2.2. Synthesis and characterization of drug loaded liposomes

Liposomes composed of HSPC, cholesterol, and DSPE-PEG2000 in a molar ratio of 58:37:5 were synthesized using the thin-film hydration (TFH) method. The total lipid concentration was about 60 μmol/ml. Briefly, components were dissolved in chloroform in a round bottom flask, and a thin film was formed by evaporating the chloroform via roto-evaporator (BUCHI R210 rotavapor, BUCHI Corporation, New Castle, DE, USA). BudP was passively loaded into the hydrophilic core during the hydration step. The thin film was then hydrated using deionized water (DI) containing 100 mg/ml of BudP, and the liposomes formed were downsized by water bath sonication (Branson 3800 ultrasonic cleaner, frequency 40 kHz, Branson cleaning Corp, Danbury, CT, USA) at 55 °C for 60 min, followed by extrusion (mini extruder, Avanti polar lipids, Birmingham, AL, USA) through 200-nm polycarbonate filters (Whatman nucleopore, Cytiva, Global Life Science Solutions LLC, Marlborough, MA, USA). The liposomes formed were dialyzed against a 50-kDa molecular weight cut-off (MWCO) membrane (Repligen, Waltham, MA, USA) for three days and six buffer exchange cycles to remove free lipids and free BudP. Liposome size, size distribution, and zeta potential were determined by dynamic light scattering using a Malvern zeta-sizer Nano-ZS (Malvern, Worcestershire, UK). Liposome batches with a polydispersity index (PDI) of less than 0.2 were considered for further experiments. The concentration of BudP entrapped in liposomes was quantified using high-performance liquid chromatography (HPLC) (Agilent, Santa Clara, CA, USA) after removing free BudP through dialysis. The liposome containing entrapped BudP was dissolved in methanol (1:9 ratio), sonicated for 10 mins, and vortexed for 30 sec. The solution was then filtered through 0.2 μm filter and analyzed using the following HPLC chromatographic conditions: mobile phase of acetonitrile: phosphate buffer (32:68) (pH 3.2), C18 column of 4.6 mm × 150 mm with 3-μm silica particles, flow rate of

Author Manuscript Author Manuscript Author Manuscript Author Manuscript

1.0 ml/min, injection volume of 50 μl, and UV wavelength of 244 nm. The encapsulation efficiency was calculated using the formula,

$$\text{encapsulation efficiency } \% = \frac{\text{Amount of BudP entrapped in liposomes after dialysis}}{\text{Amount of BudP used in synthesis}} * 100 \quad \text{(eq. 1)}$$

2.3. In vitro drug release and stability

BudP release from liposomes was measured using dialysis. One ml of L-BudP or free (F)-BudP in SBF (pH 7.4) was transferred into a dialysis tube (donor compartment) with a MWCO of 12 kDa. The dialysis tube was then suspended in 15 ml of SBF, pH 7.4 (receptor compartment), and incubated at 37 °C with agitation. The volume of the receptor medium was maintained at least ten times the donor compartment medium to maintain sink conditions. 5-ml sample was collected from the receptor compartment after 2, 4, 6, 12, 24, 48, and 72 h and replaced with fresh SBF. The BudP concentration was analyzed using the aforementioned HPLC method [24]. The colloidal stability of L-BudP was assessed in SBF at 37 °C for 7 days in terms of size and the amount of BudP present in liposomes. Samples were collected every other day for 7 days. At different time points, aliquots of the sample were collected from the donor and receptor compartments and analyzed for size and encapsulated drug content.

2.4. Animal model and experimental design

All animal procedures were performed with approval from the University of Utah Institutional Animal Care and Use Committee (IACUC protocol 21–05005). Immunocompetent, 8 to 10-week-old male BALB/c mice (Charles River Laboratories, Wilmington, MA, USA) with average weight of 22.73 ± 1.39 g, were employed to develop a mouse model of *Aspergillus fumigatus (A. fumigatus*) extract-induced CRS. A total of 60 mice were divided into five experimental groups (12 mice/group), namely control-empty liposomes (E-L; normal control / control mice), CRS-E-L (disease control / CRS mice), CRS-free BudP (F-BudP; systemic drug control), CRS-liposomal BudP (L-BudP; experimental group), and CRS-topical BudP (T-BudP; topical drug control) (Table 1). Each experimental group was further subdivided into two groups of six mice for end point analysis at 7 and 14 days after BudP treatment initiation. During model development, one unexpected death occurred in the CRS-E-L day 7 group. To generate CRS, *A. fumigatus* extracts (53,000 PNU/ml) were administered intranasally 3 times weekly for 12 weeks (Fig. 1). This model was selected to establish proof-of-concept because it generates robust and reproducible eosinophilic-associated sinonasal inflammation in mice, which has been positively correlated to treatment responsiveness to steroids in patients with eosinophilic CRS [23, 25]. Briefly, mice, with average weight of 25.02 ± 1.22 g, were anesthetized using 2.5% isoflurane, and 10 μL of *A. fumigatus* extracts in sterile PBS were administered into each nostril via a pipette. Similarly, 10 μL of sterile PBS was administered into each nostril to normal control and diseased control groups (3 × weekly, 12 weeks). Animal body weight, clinical signs (*e.g.,* changes in behavior, grooming appearance, and self-mutilation), and clinical signs associated with CRS, including appearance of nose swelling and discoloration, nose itching, sneezing, and difficulty breathing, were recorded [25, 26].

Author Manuscript Author Manuscript Author Manuscript Author Manuscript

After 12 weeks of developing CRS, E-L, F-BudP (10 mg/kg), and L-BudP (10 mg/kg) were administered via a single tail vein injection to diseased controls, systemic drug controls, and the experimental group respectively. Normal controls were injected with a single tail vein injection of E-L at similar lipid concentration. For the T-BudP treatment group, BudP was dissolved in sterile PBS and administered into each nostril using a micropipette, 5 days weekly (5 μg/nostril/dose/day) (Fig. 1). The concentration of T-BudP treatment was calculated using the following formula:

$$\text{Human Equivalent Dose} = \text{Animal Dose}\left(\frac{\text{mg}}{\text{kg}}\right) \times \left(\text{animal wt in kg/human wt in kg}\right) \text{ ^ } 0.33 \ [27] \quad \text{(eq. 2)}$$

Budesonide is the active ingredient in clinically used Rhinocort AQUA® topical nasal spray (AstraZeneca, Wilmington, DE, USA) treatment and was administered based on the human equivalent dose [28]. The amount of lipid injected was normalized between E-L and L-BudP. A known volume of L-budP solution was lyophilized to obtain the total weight of lipids + BudP. The mass of lipids was then determined by subtracting the amount of BudP present in L-BudP (obtained by HPLC analysis). The concentration of empty liposomes was adjusted to obtain similar amount of lipids. *A. fumigatus* extracts were administered to mice with CRS three times weekly following the initiation of budesonide treatments to maintain chronic inflammation.

Animals were euthanized via supratherapeutic doses of isoflurane, confirmed via toe pinch, at day 7 and day 14 after tail vein injection. At termination, whole blood was collected from the posterior vena cava and organs (*e.g.*, heart, lung, liver, kidney, and spleen) were collected for safety and efficacy evaluation. Body weight was collected throughout the study. Organ weights were measured right after euthanization. Efficacy and toxicity end points were evaluated on day 7 and day 14 after tail vein injections using a separate set of mice. Efficacy was determined through pathological examination and scoring of sinonasal tissue inflammation and immune cell influx for all study groups and compared to normal and disease controls. Toxicity was determined using body weight, organ/body weight ratio, liver enzymes in the blood, histopathological analysis of organs, and peripheral blood immune cell counts.

2.5. Histologic analysis

After euthanization, heads were separated, trimmed, and fixed in 4% neutrally buffered formalin for 48 hours. Tissues were then decalcified for two weeks in neutrally buffered 14% ethylenediaminetetraacetic acid (EDTA, pH 7.2). Fixed and decalcified tissue was then coronally sectioned at T1, T2, and T3 regions [25, 26] with the aid of surgical knives and an Olympus FSX100 stereoscope (Olympus Inc., Center Valley, PA, USA). Necropsy was performed, and organs were examined grossly, dissected, and submitted for histologic processing. The tissue sections were embedded in paraffin, and 5-μm thick slices were mounted on glass slides. The slides were either stained with hematoxylin and eosin (H&E) or left unstained for possible future studies. Paraffin embedding, sectioning, and H&E staining were performed by Associate Regional and University Pathologists laboratories

Author Manuscript Author Manuscript Author Manuscript Author Manuscript

(ARUP, Salt Lake City, UT, USA). The H&E-stained sinonasal tissues and major organs were microscopically analyzed under a BX53 clinical-grade Olympus microscope, and images were taken using a DP27 Olympus camera and Olympus cell Sense Entry 2.2 (Build 17989) imaging software by a board-certified anatomic pathologist who was blinded in terms of study design and treatment groups.

2.6. Inflammation score of sinonasal tissue

The common pathological manifestations of CRS are basement membrane thickening, goblet cell hyperplasia, subepithelial edema, immune cell infiltration, and active remodeling of damaged tissues in the sinonasal mucosa [2, 3]. The sinonasal tissues were evaluated microscopically for inflammatory changes, including basement membrane thickening, presence or absence of goblet cells, subepithelial fibrosis, squamous cell metaplasia, and inflammatory cell infiltrates [25]. Overall inflammation was graded on a semiquantitative scale as follows: normal – grade 0; mild – grade 1; medium – grade 2; moderate – grade 3; severe – grade 4 based on low power impression of the entire sample [26].

2.7. Quantification of immune cells in sinonasal tissue

The sinonasal tissue sections were also used for quantitative assessments. Eosinophils, lymphocytes, and polymorphonuclear neutrophils were counted in the most inflamed areas (hot spots) in three consecutive high-power fields using a 60X objective. Aforementioned immune cells were enumerated, and data were tabulated.

2.8. Histopathological analysis of major organs

Sections from the heart, lungs, liver, kidney, and spleen were analyzed microscopically for histopathologic abnormalities, and data were tabulated.

2.9. Liver toxicity analysis

Following euthanization, whole blood was drawn from the posterior vena cava and was allowed to clot at room temperature for 15 mins. Serum was collected by centrifugation and separating the supernatant. Samples were blinded and submitted to ARUP Laboratories (Salt Lake City, UT) to quantify the amount of alanine aminotransferase (ALT), aspartate aminotransferase (AST), and alkaline phosphatase (AP) present in blood.

2.10. Differential complete blood cell count analysis

Following euthanization, a few drops of whole blood collected from the posterior vena cava were stored in EDTA-coated tubes. Collected blood was used for complete blood count analysis using Element HT5 (Heska, Loveland, CO, USA).

2.11. Statistical analysis

Statistical comparison was conducted using a one-way Analysis of Variance followed by Dunnett's multiple comparison test to identify significantly different groups. A p-value of less than 0.05 was considered significantly different. Statistical analysis was performed using GraphPad Prism version 9.5.0 for Windows (GraphPad Software, San Diego, California, USA). All data are represented as the mean ± standard deviation for each

Author Manuscript Author Manuscript Author Manuscript Author Manuscript

treatment group. “significant” was used to describe data when calculated as statistically significant.

3. Results

3.1. Synthesis and characterization of drug-loaded liposomes

The characteristic features of synthesized L-BudP and E-L are outlined in Fig. 2A. The average diameters of both L-BudP and E-L were approximately 150 nm with a polydispersity index (PDI) of less than 0.2. There was no significant change in liposome size over 7 days (Fig. 2B). The amount of liposomal BudP at day 7 was 73.64 ± 7.33 %, showing that 26% of the drug was released at that time (Fig. 2C). Stability analysis over 7 days showed that most of the BudP was present in the liposomes (Fig. 2D).

3.2. L-BudP treatment significantly reduced CRS-associated sinonasal inflammation

Sinonasal tissues were pathologically evaluated for all animals at days 7 and 14 after BudP treatment initiation to determine the feasibility of BudP treatment to reduce CRS-associated inflammation. Fig. 3 shows representative histology of sinonasal tissues stained with H&E for each treatment group obtained at day 14. Compared to control mice, CRS mice showed variable microscopic changes to the mucosal lining, which included goblet cell hyperplasia, thickening of the basement membrane, and infiltration of immune cells (Fig. 3). All the treatment groups, F-BudP, L-BudP, and T-BudP, resulted in improved histologic alterations compared to CRS mice. Mucosal changes, including epithelial cell barrier degeneration (Fig. 3, arrow), apical blebbing (Fig. 3, arrowhead), immune cell infiltration in subepithelial region (Fig. 3), and goblet cell hyperplasia were still pronounced in mice treated with F-BudP and T-BudP compared to mice treated with L-BudP. Reductions in CRS-associated sinonasal tissue damage were most evident in the L-BudP group, where the tissue morphology was more analogous to control mice.

Overall sinonasal tissue inflammation scores were obtained for each animal through blinded evaluation by an experienced anatomical pathologist, as demonstrated in Fig. 4A. At days 7 and 14, CRS mice had a significantly higher grade of sinonasal inflammation compared to normal mice ($p<0.0001$). At day 7, a decreasing trend in inflammation across the three treatment groups was evident compared to CRS mice, although significance was not reached. At day 14, L-BudP treatment demonstrated a significant reduction in inflammation score compared to CRS mice ($p<0.01$). Importantly, the difference in scores between L-BudP and control mice was not statistically significant, suggesting that a single tail vein injection of L-BudP had prolonged therapeutic effects in reducing CRS-associated sinonasal inflammation. This finding was corroborated by further histological results demonstrating that L-BudP treatment had a marked effect on reducing sinonasal inflammation and restoring normal tissue architecture (Fig. 3 and Supplement Fig. 1). In contrast, at day 14, animals treated with F-BudP and T-BudP did not significantly reduce sinonasal inflammation compared to the CRS mice, and inflammation scores for these groups were significantly elevated compared to normal controls ($p<0.01$).

Author Manuscript Author Manuscript Author Manuscript Author Manuscript

3.3. L-BudP treatment significantly reduced immune cell infiltration into sinonasal tissue.

Tissue eosinophils, neutrophils, and lymphocytes were examined as surrogate metrics for assessing local inflammatory responses in the sinuses over the 14-day study period (Fig. 4B–D) [3, 29]. CRS mice had significantly increased numbers of eosinophils and neutrophils within the sinonasal tissues when compared to normal controls at days 7 and 14 ($p<0.0001$), consistent with the presence of active injury and confirming the development of CRS in the experimental animals.

At day 7, tissue eosinophil numbers showed a significant percent decrease of 81.5%, 96.0%, and 64.0% in animals treated with F-BudP (9.17±10.53), L-BudP (2.00±1.26) and T-BudP (17.83±12.22), respectively (Fig. 4B) compared to the CRS group (49.60±41.19) ($p<0.05$ for three treatments). At day 14, the eosinophil counts for L-BudP (9.00±8.05) and T-BudP (9.17±8.80) treatment was significantly lower compared to CRS mice (35.00±18.93) ($p<0.001$ for L-BudP and T-BudP). Notably, the eosinophil counts for F-BudP (29.83±12.01) treatment group and CRS mice was similar. The eosinophil numbers for L-BudP and T-BudP treatment were comparable to control mice, while F-BudP treatment was significantly higher than control mice ($p<0.0001$).

At day 7, tissue neutrophil numbers (Fig. 4C), were significantly lower for F-BudP (35.33±29.80), L-BudP (24.17±21.08) and T-BudP (57.17±18.76) treatment groups compared to CRS mice (140±84.73) ($p<0.05$ for three treatments). All treatments were not significantly different from control mice (4.67±5.57). On day 14, L-BudP (36±25.39) and T-BudP (64.33±37.91) treatments significantly reduced the neutrophil numbers compared to CRS mice (140.33±73.03) ($p<0.05$ for L-BudP and $p<0.01$ for T-BudP). F-Budp treatment (99.83±36.32) failed to lower the neutrophils number compared to CRS mice. Compared to control mice (11.17±12.14), the tissue neutrophil number for L-BudP and T-BudP treatments were similar, while F-BudP was significantly higher. For tissue lymphocyte number (Fig. 4D), L-BudP (28.17±12.53) and T-BudP (27±15.39) treatment reduced the lymphocyte counts on day 7 compared to CRS mice (71.20±44.88) ($p<0.05$ for L-BudP and T-BudP). F-BudP (46.67±22.52) treatment was not significantly different compared to CRS mice. On day 14, lymphocyte counts for all treatment groups were not significantly different from those for CRS and control groups (Fig. 4D).

3.4. BudP treatment transiently impacted body and organ weight

Body weights were measured daily to evaluate the potential gross toxicity associated with BudP treatment. Steroid-naive animals (control E-L and CRS E-L) did not experience changes in body weight over the 14-day observation period (Fig. 5). In contrast, all three BudP treatment groups experienced reductions in body weight over the treatment period, with the most pronounced reductions occurring within the first week of treatment. By the end of the study period at day 14, all animals had reached 90.81±1.39 %, 87.51±1.11%, and 93.65±1.17% of their initial body weight for F-BudP, L-BudP, and T-BudP, respectively. The body weight for T-BudP treatment plateaued until day 14. The body weight for both, F-BudP and L-BudP treatment gradually started improving and was comparable to T-BudP treatment at day 14. The statistical analysis of the data set is displayed in Supplement Table 1.

Author Manuscript Author Manuscript Author Manuscript Author Manuscript

Organ-to-body weight ratios were calculated for all animals at days 7 and 14 to evaluate the impact of BudP treatment on the liver, kidneys, and spleen (Fig. 6). Corticosteroids are heavily metabolized by cytochrome P450 liver enzymes [30]. At day 7, the liver to body weight ratio calculated for T-BudP treatment showed a significant increase from controls (*p <0.05). At day 14, the liver to body weight ratio for L-BudP (***p<0.001) and T-BudP treatment (*p<0.05) were significantly different from controls (Fig. 6). Kidneys play a crucial role in the excretion of corticosteroids [31]. The difference observed in kidney to body weight ratio at day 7 in F-BudP (****p<0.0001), L-BudP (****p<0.0001) and T-BudP treatment (*p<0.05) were reduced at day 14, implying that BudP excretion occurred mostly within the first week (Fig. 6). The spleen plays a vital role of controlling the level of WBC's [32]. The spleen/body weight ratio was significantly lower in all three-treatment groups compared to control mice at day 7. While, at day 14 there was no significant difference between treatment groups (Fig. 6). Comparison of organ-to-body weight ratio for heart and lung was difficult to compare; for some animals, organs were completely saturated with blood during necropsy, confounding the actual weight values. The differences observed in body weight and organ-to-body weight ratios was further combined with histopathological observation of organ tissues to confirm the presence of any toxicity in different organs (Section 3.6).

3.5. BudP treatment alters systemic liver enzyme concentration

The amount of liver enzymes in the blood was analyzed to identify potential BudP-induced toxicity or stress associated with the liver. The normal limits for ALT (41 to 131 U/L), AST(55 to 352 U/L) and AP(118 to 433 U/L) for BALB/c mice [33] are denoted by upper limit (UL), and lower limit (LL) in Fig. 7A–C. ALT was within normal limits with the F-BudP (***p<0.001) treatment group noted to be slightly elevated at day 7 compared to control mice (Fig. 7A). AST levels with different treatments were not significantly different from control mice at both the 7- and 14-day timepoints and were within the normal limit (Fig. 7B). The level of AP in blood was reduced due to BudP treatment but starting to recover at the later timepoint (Fig. 7C).

3.6. BudP treatment-associated toxicity was not found in the histopathological analysis of major organs

Histopathological analysis of heart, lung, liver, kidneys, and spleen showed minimal microscopic alterations in animals treated with BudP. These microscopic findings were limited and did not show a clear association with a specific treatment group. Mild to moderate inflammatory changes were found in the lower airways from CRS mice, irrespective of the treatment groups. The observed changes included mixed perivascular and peri-bronchial inflammation composed of lymphocytes, plasma cells, neutrophils and eosinophils (Supplement Fig 2). Comparable changes were previously described in similar experimental animal models [34]. Notably, no significant inflammation was present in pulmonary tissues obtained from control animals.

3.7. BudP treatment induces transient changes in peripheral blood immune cell counts

Corticosteroids are known to transiently affect the distribution of white blood cell (WBC) percentages in patients [35–38]. Complete blood cell count analyses were conducted on

Author Manuscript Author Manuscript Author Manuscript Author Manuscript

days 7 and 14 after the initiation of treatment (Fig. 8A, B). F-BudP and L-BudP treatment lowered the lymphocyte and increased neutrophil counts compared to normal controls (Fig. 8A, B). The normal limits for neutrophils (9.86% to 39.11% of total WBCs) and lymphocytes (48.81% to 83.19% of total WBCs) for BALB/c mice [39] are denoted by upper limit (UL) and lower limit (LL) in Fig. 8A, B. Neutrophil counts at day 7 suggest that L-BudP and F-BudP treatment resulted in a significant increase in a system response compared to normal controls. However, by day 14, these values approached those determined for normal controls and fell within the normal range, with a similar trend observed for lymphocytes.

4. Discussion

Liposomes have been shown to increase drug circulation half-life and accumulation at the target site in various preclinical inflammatory models [19, 40–42], including sinonasal tissue accumulation in mice with CRS [23]. Our main objective in this investigation was to evaluate if drug-loaded liposomes in a single injection could be utilized to reduce inflammation in the sinonasal mucosa while limiting systemic toxicity of BudP in a murine model of CRS compared to daily T-BudP treatment. The results of this proof-of-concept study demonstrate that a single injection of L-BudP (10 mg/kg) enhanced and sustained efficacy in reducing the inflammation in sinonasal tissue up to 14 days compared to both F-BudP (10 mg/kg) and T-BudP (5 μg/nostril/dose/day). The equivalent dose of F-BudP and T-BudP (calculated from clinical dosing) failed to provide prolonged efficacy, and the disease remission obtained was suboptimal. The toxicity observed with L-BudP treatment was minimal and transient and was comparable to the T-BudP mice. Suggesting that liposomes can be used to increase the efficacy of corticosteroids, while maintaining a low toxicity profile in treating CRS.

E-L and L-BudP liposomes had an average diameter of approximately 150 nm (Fig. 2B, C). The size of the liposome was selected based on our prior study that reported the accumulation and retention of 150-nm PEGylated liposomes in *A. fumigatus* extract-induced CRS in mice [23]. This size is adequate for extravasation through the leaky blood vessels, likely caused by sinonasal tissue vascular dysregulation observed in CRS [22, 43]. The encapsulation efficacy of BudP was approximately ~4% (data not shown), indicating that loading efficiency could be improved. The stability and *in vitro* drug release studies showed that L-BudP is stable, and the release of BudP from the liposomes was minimal at around 26% until day 7 (Fig. 2E). PEG2000 was incorporated in the liposomal surface to delay uptake by mononuclear phagocytic system, thereby increasing the circulation half-life [44, 45].

CRS is characterized by immune cell infiltration and sinonasal epithelial cell barrier degeneration [2]. Immune cells, such as eosinophils, neutrophils, and lymphocytes, play an active role in modulating inflammation in CRS [46]. A single injection of L-BudP treatment resulted in a persistent reduction in eosinophil, neutrophil, and lymphocyte infiltrates into the sinuses over the 14-day study period. The prolonged decrease in immune cells observed with L-BudP treatment is likely due to the improved circulation half-life and subsequent increased passive accumulation of BudP at the inflamed site by extravasation

Author Manuscript Author Manuscript Author Manuscript Author Manuscript

of liposomes through leaky vasculature [47]. After extravasation, L-BudP either releases BudP or becomes sequestered by active immune cells, leading to the downregulating pro-inflammatory cytokines, chemokines, and tissue-degrading enzymes [47] [48]. Reduction in pro-inflammatory agents within the inflamed tissue, in turn, leads to decreased immune cell chemotaxis [35, 49, 50]. Thus, the reduction in immune cells observed with F-BudP treatment is transient due to the short half-life and low bioavailability of freely circulating BudP [28]. In other inflammatory conditions, liposomal corticosteroids have shown a prolonged decrease in immune cell infiltration into inflamed target tissues compared to free drugs [19, 51, 52]. Prolonged reduction in immune cell infiltration into inflamed tissue is the first step in controlling inflammation and can translate into mucosal healing.

Evidence of CRS remission was observed in all animals treated with BudP. Yet, the evidence was more pronounced in animals treated with a single injection of L-BudP (Fig. 3). The enhanced efficacy observed with L-BudP is due to prolonged reduction in immune cells combined with upregulation of anti-inflammatory cytokines, leading to the removal of cell debris and tissue repair [53]. The presence of epithelial cell injury, apical blebbing, goblet cell hyperplasia, and immune cell infiltration was still present in the F-BudP and T-BudP treatment groups (Fig. 3). The overall Inflammation score after L-BudP treatment was similar to that of control mice at day 14. Inflammation scores for F-BudP and T-BudP treatments were still not different from CRS mice (Fig. 4A). Taken together, these results suggest that L-BudP treatment is efficient in maintaining the therapeutic concentration of BudP at the sinonasal tissue for an extended time evidenced by the induction of robust anti-inflammatory effects and histological remission. Enhanced histological remissions have been observed when liposomal corticosteroids were used in treatment of other inflammatory conditions, such as rheumatoid arthritis [19, 52], inflammatory liver disease [54], and multiple sclerosis [51], compared to free corticosteroids. We believe, the PEGylated liposomal system assists in prolonging the anti-inflammatory effect of corticosteroids compared to free drugs, which could potentially translate into reduced dosing frequency in patients with CRS. Although administered daily, T-BudP treatment did not result in significant disease remission. The amount of BudP reaching the epithelial layer might be limited and not uniform, which is consistent with current literature highlighting the drawbacks of topical treatment, such as mucociliary clearance, physical and anatomical barriers [6]. Thus, L-BudP treatment is more advantageous for sustained reduction of immune cell influx and causes tissue remission in the sinonasal tissue of CRS.

In a rheumatoid arthritis animal model, Anderson et al. [44] showed immune cell reduction and histological tissue remission using liposomal dexamethasone phosphate (L-DEXP) at a 10-fold lower dose compared to free DEXP. Similarly, Hoven *et al.* [55] and Hofkens *et al.* [45] studied the efficacy and safety of highly potent GCs and compared them with prednisolone. The therapeutic efficacy observed with liposomal prednisolone phosphate was achieved with 1/5 and 1/10 of the concentration of L-DEXP and L-BudP, respectively. These studies support that liposomal corticosteroid systems effectively control inflammation at a lower concentration than their free drug counterpart. In the current study, the concentration of BudP used was 10-fold higher than that used by Hoven et al. [55] Thus, in future studies a lower concentration of BudP will be evaluated.

Author Manuscript Author Manuscript Author Manuscript Author Manuscript

Changes in body weight, organ-to-body weight ratio, liver enzyme levels, and systemic immune cells are conventional metrics by which drug toxicity can be assessed [45, 56]. As expected, E-L treatment showed no reduction in the body weights of normal and CRS controls over the 14-day study period (Fig. 5). T-BudP treatment showed a continuous reduction in body weight until day 14 (Fig. 5), indicating systemic absorption of BudP. F-BudP and L-BudP treatment resulted in a continuous loss in body weight until day 7 (Fig. 5) with a near-return to baseline by day 14. Transient reduction in body weight after systemic administration of liposomal corticosteroids is a known phenomenon attributed to the small fraction of systemic drug leakage [42, 52, 55]. Hoven *et al.* [55] reported that 1 mg/kg of L-BudP did not cause body weight reduction. Thus, a temporary reduction in body weight observed in this study could be further mitigated by lowering the BudP concentration. Transient reduction in organ weights was observed, but the histology of all the organs showed no significant inflammation that could be associated with the treatments at both time points, indicating that the treatments were well tolerated.

Lymphopenia and neutrophilia are other common adverse effects observed with liposomal corticosteroid treatment in preclinical models [52, 57]. In this study, differential immune cell quantification in peripheral blood showed a transient increase in neutrophils and a reduction in lymphocyte counts. The increase in neutrophils is likely due to reduced cell adhesion, leading to accumulation in the peripheral circulation [36]. The reduction in lymphocyte count in peripheral blood may be due to redistribution to lymphoid organs or by directly affecting proliferation [35]. These changes in circulating immune cells are transient and well-documented with oral corticosteroid [37, 38, 58] and liposomal corticosteroid treatments [52, 57]. Both the neutrophil and lymphocyte concentrations were approaching normal levels at day 14 (Fig. 8A, B), which is consistent with previous reports. Nevertheless, the impact of the brief changes in systemic immune cells should be further evaluated for susceptibility to opportunistic infection in future experiments. The transient toxicity observed in this study is associated with the concentration of BudP, as a similar level of toxicity is found with F-BudP treatment and is absent with E-L treatment. A single injection of L-BudP treatment has enhanced efficacy compared to a single injection of F-BudP or repeat daily administration of T-BudP, while showing similar toxicity to T-BudP. Thus, delivering corticosteroids by liposomes can provide a beneficial role in treating patients with CRS compared to topical treatments.

We acknowledge several limitations in our study design for consideration when interpreting the results. The concentration of BudP injected was selected based on a pilot toxicity study data (supplement Fig 3, 4). Dose escalation studies to optimize BudP concentration and to determine the ideal balance between BudP-induced efficacy and toxicity are ongoing. The toxicity profiles of F-BudP and L-BudP will be different due to their difference in circulation half-lives. In our current study, toxicity was determined only at the efficacy end points. To better understand both acute and prolonged toxicity profiles of BudP, more timepoints and an extended study period beyond 14 days should be examined. The pharmacological and molecular mechanisms through which L-BudP treatment results in enhanced efficacy for a prolonged period after a single dose injection are not clearly understood. Mechanistic investigations such as cell uptake studies paired with *in vivo* distribution should be conducted to help understand the molecular mechanisms involved in enhanced efficacy.

Author Manuscript Author Manuscript Author Manuscript Author Manuscript

Future studies should focus on determining the biodistribution and pharmacokinetics of BudP after L-BudP treatment and should include comparison of different corticosteroids to determine the appropriate drug for reducing inflammation in CRS. Despite these limitations, results from this study show promise for the utility of liposomal carriers in delivering corticosteroids for improved efficacy while lowering systemic toxicity in the prolonged treatment of CRS.

5. Conclusion

A liposomal system improved the efficacy of corticosteroids in treating CRS-associated sinonasal inflammation. In our cohort, L-BudP treatment was superior to F- and T-BudP in reducing sinonasal mucosal injury for a prolonged period of time. The efficacy observed through F-BudP and T-BudP were short-lived and suboptimal, respectively. The toxicity associated with L-BudP was transient and comparable to current standard of care (T-BudP). The improved efficacy observed through L-BudP is likely attributed to increased circulation half-life and increased passive accumulation at the inflamed sinonasal tissue. The lasting efficacy could potentially be translated into less frequent dosing of corticosteroids in patients with a favorable toxicity profile, thus improving patient compliance and lowering associated adverse effects.

Supplementary Material

Refer to Web version on PubMed Central for supplementary material.

Acknowledgement

This research was funded by the Skaggs Graduate Research Fellowship, awarded by the University of Utah, College of Pharmacy (B.Y.), a Research Incentive Seed Grant, awarded by the University of Utah School of Medicine (J.A), and grant R44AI126987, awarded by the National Institute of Allergy and Infectious Diseases (A.P.). Research reported in this publication was supported by the National Center for Advancing Translational Sciences of the National Institutes of Health under Award Numbers UM1TR004409 and 1K12TR004413. The authors would like to thank the Preclinical Research Resource at the Huntsman Cancer Institute at the University of Utah, supported by the National Cancer Institute of the National Institutes of Health under Award Number P30CA042014, for their assistance in conducting the *in vivo* CRS model. The content is solely the responsibility of the authors and does not necessarily represent the official views of the NIH. The authors would like to thank Chelsea Pollard for her contributions to animal studies.

Reference

[1]. Palmer JN, Messina JC, Biletch R, Grosel K, Mahmoud RA, A cross-sectional, population-based survey of U.S. adults with symptoms of chronic rhinosinusitis, Allergy Asthma Proc, 40 (2019) 48–56. [PubMed: 30582496]

[2]. Orlandi RR, Kingdom TT, Smith TL, Bleier B, DeConde A, Luong AU, Poetker DM, Soler Z, Welch KC, Wise SK, Adappa N, Alt JA, Anselmo-Lima WT, Bachert C, Baroody FM, Batra PS, Bernal-Sprekelsen M, Beswick D, Bhattacharyya N, Chandra RK, Chang EH, Chiu A, Chowdhury N, Citardi MJ, Cohen NA, Conley DB, DelGaudio J, Desrosiers M, Douglas R, Eloy JA, Fokkens WJ, Gray ST, Gudis DA, Hamilos DL, Han JK, Harvey R, Hellings P, Holbrook EH, Hopkins C, Hwang P, Javer AR, Jiang RS, Kennedy D, Kern R, Laidlaw T, Lal D, Lane A, Lee HM, Lee JT, Levy JM, Lin SY, Lund V, McMains KC, Metson R, Mullol J, Naclerio R, Oakley G, Otori N, Palmer JN, Parikh SR, Passali D, Patel Z, Peters A, Philpott C, Psaltis AJ, Ramakrishnan VR, Ramanathan M, Roh HJ, Rudmik L, Sacks R, Schlosser RJ, Sedaghat AR, Senior BA, Sindwani R, Smith K, Snidvongs K, Stewart M, Suh JD, Tan BK, Turner JH, van Drunen CM, Voegels R, Wang Y, Woodworth BA, Wormald PJ, Wright ED, Yan C, Zhang

Author Manuscript Author Manuscript Author Manuscript Author Manuscript

L, Zhou B, International consensus statement on allergy and rhinology: rhinosinusitis 2021, Int Forum Allergy Rhinol, 11 (2021) 213–739. [PubMed: 33236525]

[3]. Fokkens WJ, Lund VJ, Hopkins C, Hellings PW, Kern R, Reitsma S, Toppila-Salmi S, Bernal-Sprekelsen M, Mullol J, Alobid I, Terezinha Anselmo-Lima W, Bachert C, Baroody F, von Buchwald C, Cervin A, Cohen N, Constantinidis J, De Gabory L, Desrosiers M, Diamant Z, Douglas RG, Gevaert PH, Hafner A, Harvey RJ, Joos GF, Kalogjera L, Knill A, Kocks JH, Landis BN, Limpens J, Lebeer S, Lourenco O, Meco C, Matricardi PM, O'Mahony L, Philpott CM, Ryan D, Schlosser R, Senior B, Smith TL, Teeling T, Tomazic PV, Wang DY, Wang D, Zhang L, Agius AM, Ahlstrom-Emanuelsson C, Alabri R, Albu S, Alhabash S, Aleksic A, Aloulah M, Al-Qudah M, Alsaleh S, Baban MA, Baudoin T, Balvers T, Battaglia P, Bedoya JD, Beule A, Bofares KM, Braverman I, Brozek-Madry E, Richard B, Callejas C, Carrie S, Caulley L, Chussi D, de Corso E, Coste A, El Hadi U, Elfarouk A, Eloy PH, Farrokhi S, Felisati G, Ferrari MD, Fishchuk R, Grayson W, Goncalves PM, Grdinic B, Grgic V, Hamizan AW, Heinichen JV, Husain S, Ping TI, Ivaska J, Jakimovska F, Jovancevic L, Kakande E, Kamel R, Karpischenko S, Kariyawasam HH, Kawauchi H, Kjeldsen A, Klimek L, Krzeski A, Kopacheva Barsova G, Kim SW, Lal D, Letort JJ, Lopatin A, Mahdjoubi A, Mesbahi A, Netkovski J, Nyenbue Tshipukane D, Obando-Valverde A, Okano M, Onerci M, Ong YK, Orlandi R, Otori N, Ouennoughy K, Ozkan M, Peric A, Plzak J, Prokopakis E, Prepageran N, Psaltis A, Pugin B, Raftopulos M, Rombaux P, Riechelmann H, Sahtout S, Sarafoleanu CC, Searyoh K, Rhee CS, Shi J, Shkoukani M, Shukuryan AK, Sicak M, Smyth D, Sindvongs K, Soklic Kosak T, Stjarne P, Sutikno B, Steinsvag S, Tantilipikorn P, Thanaviratananich S, Tran T, Urbancic J, Valiulius A, Vasquez de Aparicio C, Vicheva D, Virkkula PM, Vicente G, Voegels R, Wagenmann MM, Wardani RS, Welge-Lussen A, Witterick I, Wright E, Zabolotniy D, Zsolt B, Zwetsloot CP, European Position Paper on Rhinosinusitis and Nasal Polyps 2020, Rhinology, 58 (2020) 1–464.

[4]. Moffa A, Costantino A, Rinaldi V, Sabatino L, Trecca EMC, Baptista P, Campisi P, Cassano M, Casale M, Nasal Delivery Devices: A Comparative Study on Cadaver Model, Biomed Res Int, 2019 (2019) 4602651. [PubMed: 31032346]

[5]. Thomas WW, Harvey RJ, Rudmik L, Hwang PH, Schlosser RJ, Distribution of topical agents to the paranasal sinuses: an evidence-based review with recommendations, Int Forum Allergy Rhinol, 3 (2013) 691–703. [PubMed: 23729216]

[6]. Schilling AL, Cannon E, Lee SE, Wang EW, Little SR, Advances in controlled drug delivery to the sinonasal mucosa, Biomaterials, 282 (2022) 121430. [PubMed: 35202932]

[7]. Tait S, Kallogjeri D, Suko J, Kukuljan S, Schneider J, Piccirillo JF, Effect of Budesonide Added to Large-Volume, Low-pressure Saline Sinus Irrigation for Chronic Rhinosinusitis: A Randomized Clinical Trial, JAMA Otolaryngol Head Neck Surg, 144 (2018) 605–612. [PubMed: 29879268]

[8]. Bachert C, Holtappels G, Pathophysiology of chronic rhinosinusitis, pharmaceutical therapy options, GMS Curr Top Otorhinolaryngol Head Neck Surg, 14 (2015) Doc09.

[9]. Head K, Chong LY, Hopkins C, Philpott C, Schilder AG, Burton MJ, Short-course oral steroids as an adjunct therapy for chronic rhinosinusitis, Cochrane Database Syst Rev, 4 (2016) CD011992.

[10]. Howard BE, Lal D, Oral steroid therapy in chronic rhinosinusitis with and without nasal polyposis, Curr Allergy Asthma Rep, 13 (2013) 236–243. [PubMed: 23225105]

[11]. Poetker DM, Oral corticosteroids in the management of chronic rhinosinusitis with and without nasal polyps: Risks and benefits, Am J Rhinol Allergy, 29 (2015) 339–342. [PubMed: 26358344]

[12]. Leopold DA, Elkayam D, Messina JC, Kosik-Gonzalez C, Djupesland PG, Mahmoud RA, NAVIGATE II: Randomized, double-blind trial of the exhalation delivery system with fluticasone for nasal polyposis, J Allergy Clin Immunol, 143 (2019) 126–134.e125. [PubMed: 29928924]

[13]. Manji J, Singh G, Okpaleke C, Dadgostar A, Al-Asousi F, Amanian A, Macias-Valle L, Finkelstein A, Tacey M, Thamboo A, Javer A, Safety of long-term intranasal budesonide delivered via the mucosal atomization device for chronic rhinosinusitis, Int Forum Allergy Rhinol, 7 (2017) 488–493. [PubMed: 28151588]

[14]. Tai J, Lee K, Kim TH, Current Perspective on Nasal Delivery Systems for Chronic Rhinosinusitis, Pharmaceutics, 13 (2021).

[15]. Habib AR, Thamboo A, Manji J, Dar Santos RC, Gan EC, Anstead A, Javer AR, The effect of head position on the distribution of topical nasal medication using the Mucosal Atomization Device: a cadaver study, Int Forum Allergy Rhinol, 3 (2013) 958–962. [PubMed: 24106231]

Author Manuscript Author Manuscript Author Manuscript Author Manuscript

[16]. Lee M, Park CG, Huh BK, Kim SN, Lee SH, Khalmuratova R, Park JW, Shin HW, Choy YB, Sinonasal Delivery of Resveratrol via Mucoadhesive Nanostructured Microparticles in a Nasal Polyp Mouse Model, Sci Rep, 7 (2017) 40249. [PubMed: 28071713]

[17]. Pandey P, Cabot PJ, Wallwork B, Panizza BJ, Parekh HS, Formulation, functional evaluation and ex vivo performance of thermoresponsive soluble gels - A platform for therapeutic delivery to mucosal sinus tissue, Eur J Pharm Sci, 96 (2017) 499–507. [PubMed: 27771516]

[18]. Schilling AL, Kulahci Y, Moore J, Wang EW, Lee SE, Little SR, A thermoresponsive hydrogel system for long-acting corticosteroid delivery into the paranasal sinuses, J Control Release, 330 (2021) 889–897. [PubMed: 33157189]

[19]. Hofkens W, Grevers LC, Walgreen B, de Vries TJ, Leenen PJ, Everts V, Storm G, van den Berg WB, van Lent PL, Intravenously delivered glucocorticoid liposomes inhibit osteoclast activity and bone erosion in murine antigen-induced arthritis, J Control Release, 152 (2011) 363–369. [PubMed: 21396411]

[20]. Ren K, Yuan H, Zhang Y, Wei X, Wang D, Macromolecular glucocorticoid prodrug improves the treatment of dextran sulfate sodium-induced mice ulcerative colitis, Clin Immunol, 160 (2015) 71–81. [PubMed: 25869296]

[21]. Jia Z, Wang X, Wei X, Zhao G, Foster KW, Qiu F, Gao Y, Yuan F, Yu F, Thiele GM, Bronich TK, O'Dell JR, Wang D, Micelle-Forming Dexamethasone Prodrug Attenuates Nephritis in Lupus-Prone Mice without Apparent Glucocorticoid Side Effects, ACS Nano, 12 (2018) 7663–7681. [PubMed: 29965725]

[22]. Khurana N, Pulsipher A, Jedrzkiewicz J, Ashby S, Pollard CE, Ghandehari H, Alt JA, Inflammation-driven vascular dysregulation in chronic rhinosinusitis, Int Forum Allergy Rhinol, (2020).

[23]. Khurana N, Yathavan B, Jedrzkiewicz J, Gill AS, Pulsipher A, Alt JA, Ghandehari H, Vascular permeability in chronic rhinosinusitis enhances accumulation and retention of nanoscale pegylated liposomes, Nanomedicine, 38 (2021) 102453. [PubMed: 34363985]

[24]. Ren H, He Y, Liang J, Cheng Z, Zhang M, Zhu Y, Hong C, Qin J, Xu X, Wang J, Role of Liposome Size, Surface Charge, and PEGylation on Rheumatoid Arthritis Targeting Therapy, ACS Appl Mater Interfaces, 11 (2019) 20304–20315. [PubMed: 31056910]

[25]. Alt JA, Lee WY, Davis BM, Savage JR, Kennedy TP, Prestwich GD, Pulsipher A, A synthetic glycosaminoglycan reduces sinonasal inflammation in a murine model of chronic rhinosinusitis, PLOS ONE, 13 (2018) e0204709. [PubMed: 30252910]

[26]. Lindsay R, Slaughter T, Britton-Webb J, Mog SR, Conran R, Tadros M, Earl N, Fox D, Roberts J, Bolger WE, Development of a murine model of chronic rhinosinusitis, Otolaryngol Head Neck Surg, 134 (2006) 724–730; discussion 731–722. [PubMed: 16647523]

[27]. Nair AB, Jacob S, A simple practice guide for dose conversion between animals and human, J Basic Clin Pharm, 7 (2016) 27–31. [PubMed: 27057123]

[28]. Rhinocort [Package insert]. Wilmington, DE. AstraZeneca. 1999, in.

[29]. Fokkens WJ, Lund VJ, Mullol J, Bachert C, Alobid I, Baroody F, Cohen N, Cervin A, Douglas R, Gevaert P, Georgalas C, Goossens H, Harvey R, Hellings P, Hopkins C, Jones N, Joos G, Kalogjera L, Kern B, Kowalski M, Price D, Riechelmann H, Schlosser R, Senior B, Thomas M, Toskala E, Voegels R, Wang d.Y., Wormald PJ, European Position Paper on Rhinosinusitis and Nasal Polyps 2012, Rhinol Suppl, 23 (2012) 3 p preceding table of contents, 1–298. [PubMed: 22764607]

[30]. Jönsson G, Aström A, Andersson P, Budesonide is metabolized by cytochrome P450 3A (CYP3A) enzymes in human liver, Drug Metab Dispos, 23 (1995) 137–142. [PubMed: 7720517]

[31]. Abdalla MI, Herfarth H, Budesonide for the treatment of ulcerative colitis, Expert Opin Pharmacother, 17 (2016) 1549–1559. [PubMed: 27157244]

[32]. Lewis SM, Williams A, Eisenbarth SC, Structure and function of the immune system in the spleen, Sci Immunol, 4 (2019).

[33]. BALB/C Mouse Biochemistry. North American Colonies. January 2008-December 2012. Charles River Laboratories International, Inc. Website accessed - April 19, 2023. chrome-extension://efaidnbmnnnibpcajpcglclefindmkaj/https://www.criver.com/sites/default/files/resources/doc_a/BALBcMouseClinicalPathologyData.pdf, in.

Author Manuscript Author Manuscript Author Manuscript Author Manuscript

[34]. Hoselton SA, Samarasinghe AE, Seydel JM, Schuh JM, An inhalation model of airway allergic response to inhalation of environmental Aspergillus fumigatus conidia in sensitized BALB/c mice, Med Mycol, 48 (2010) 1056–1065. [PubMed: 20482452]

[35]. Spahn JD, Landwehr LP, Nimmagadda S, Surs W, Leung DY, Szefler SJ, Effects of glucocorticoids on lymphocyte activation in patients with steroid-sensitive and steroid-resistant asthma, J Allergy Clin Immunol, 98 (1996) 1073–1079. [PubMed: 8977508]

[36]. Clark RA, Gallin JI, Fauci AS, Effects of in vivo prednisone on in vitro eosinophil and neutrophil adherence and chemotaxis, Blood, 53 (1979) 633–641. [PubMed: 426911]

[37]. Stark JG, Werner S, Homrighausen S, Tang Y, Krieg M, Derendorf H, Moellmann H, Hochhaus G, Pharmacokinetic/pharmacodynamic modeling of total lymphocytes and selected subtypes after oral budesonide, J Pharmacokinet Pharmacodyn, 33 (2006) 441–459. [PubMed: 16633890]

[38]. Yu DT, Clements PJ, Paulus HE, Peter JB, Levy J, Barnett EV, Human lymphocyte subpopulations. Effect of corticosteroids, J Clin Invest, 53 (1974) 565–571. [PubMed: 11344571]

[39]. BALB/C Mouse Hematology. North American Colonies. January 2008-December 2012. Charles River Laboratories International, Inc. Website accessed - April 19, 2023. chrome-extension://efaidnbmnnnibpcajpcglclefindmkaj/https://www.criver.com/sites/default/files/resources/doc_a/BALBcMouseClinicalPathologyData.pdf, in.

[40]. Wong C, Bezhaeva T, Rothuizen TC, Metselaar JM, de Vries MR, Verbeek FPR, Vahrmeijer AL, Wezel A, van Zonneveld A-J, Rabelink TJ, Quax PHA, Rotmans JI, Liposomal prednisolone inhibits vascular inflammation and enhances venous outward remodeling in a murine arteriovenous fistula model, Scientific Reports, 6 (2016) 30439. [PubMed: 27460883]

[41]. Jubeh TT, Nadler-Milbauer M, Barenholz Y, Rubinstein A, Local treatment of experimental colitis in the rat by negatively charged liposomes of catalase, TMN and SOD, J Drug Target, 14 (2006) 155–163. [PubMed: 16753829]

[42]. Metselaar JM, Wauben MH, Wagenaar-Hilbers JP, Boerman OC, Storm G, Complete remission of experimental arthritis by joint targeting of glucocorticoids with long-circulating liposomes, Arthritis Rheum, 48 (2003) 2059–2066. [PubMed: 12847701]

[43]. Khurana N, Pulsipher A, Ghandehari H, Alt JA, Meta-analysis of global and high throughput public gene array data for robust vascular gene expression discovery in chronic rhinosinusitis: Implications in controlled release, J Control Release, (2020).

[44]. Bulbake U, Doppalapudi S, Kommineni N, Khan W, Liposomal Formulations in Clinical Use: An Updated Review, Pharmaceutics, 9 (2017).

[45]. Hofkens W, van den Hoven JM, Pesman GJ, Nabbe KC, Sweep FC, Storm G, van den Berg WB, van Lent PL, Safety of glucocorticoids can be improved by lower yet still effective dosages of liposomal steroid formulations in murine antigen-induced arthritis: comparison of prednisolone with budesonide, Int J Pharm, 416 (2011) 493–498. [PubMed: 21382459]

[46]. Hulse KE, Immune Mechanisms of Chronic Rhinosinusitis, Curr Allergy Asthma Rep, 16 (2016) 1. [PubMed: 26677109]

[47]. Metselaar JM, van den Berg WB, Holthuysen AE, Wauben MH, Storm G, van Lent PL, Liposomal targeting of glucocorticoids to synovial lining cells strongly increases therapeutic benefit in collagen type II arthritis, Ann Rheum Dis, 63 (2004) 348–353. [PubMed: 15020326]

[48]. Iborra M, Alvarez-Sotomayor D, Nos P, Long-term safety and efficacy of budesonide in the treatment of ulcerative colitis, Clin Exp Gastroenterol, 7 (2014) 39–46. [PubMed: 24523594]

[49]. Rawla P, Sunkara T, Thandra KC, Gaduputi V, Efficacy and Safety of Budesonide in the Treatment of Eosinophilic Esophagitis: Updated Systematic Review and Meta-Analysis of Randomized and Non-Randomized Studies, Drugs R D, 18 (2018) 259–269. [PubMed: 30387081]

[50]. Schett G, Neurath MF, Resolution of chronic inflammatory disease: universal and tissue-specific concepts, Nat Commun, 9 (2018) 3261. [PubMed: 30111884]

[51]. Schmidt J, Metselaar MHM Jm Fau - Wauben, Wauben KV Mh Fau - Toyka, Toyka G Kv Fau - Storm, Storm R G Fau - Gold, Gold R, Drug targeting by long-circulating liposomal glucocorticosteroids increases therapeutic efficacy in a model of multiple sclerosis, Brain:a journal of neurology, (2003) 1895–1904. [PubMed: 12805101]

Author Manuscript Author Manuscript Author Manuscript Author Manuscript

[52]. Anderson R, Franch A, Castell M, Perez-Cano FJ, Bräuer R, Pohlers D, Gajda M, Siskos AP, Katsila T, Tamvakopoulos C, Rauchhaus U, Panzner S, Kinne RW, Liposomal encapsulation enhances and prolongs the anti-inflammatory effects of water-soluble dexamethasone phosphate in experimental adjuvant arthritis, Arthritis Res Ther, 12 (2010) R147. [PubMed: 20642832]

[53]. Barnes PJ, How corticosteroids control inflammation: Quintiles Prize Lecture 2005, Br J Pharmacol, 148 (2006) 245–254. [PubMed: 16604091]

[54]. Bartneck M, Scheyda KM, Warzecha KT, Rizzo LY, Hittatiya K, Luedde T, Storm G, Trautwein C, Lammers T, Tacke F, Fluorescent cell-traceable dexamethasone-loaded liposomes for the treatment of inflammatory liver diseases, Biomaterials, 37 (2015) 367–382. [PubMed: 25453965]

[55]. van den Hoven JM, Hofkens W, Wauben MH, Wagenaar-Hilbers JP, Beijnen JH, Nuijen B, Metselaar JM, Storm G, Optimizing the therapeutic index of liposomal glucocorticoids in experimental arthritis, Int J Pharm, 416 (2011) 471–477. [PubMed: 21440612]

[56]. Sellers RS, Morton D, Michael B, Roome N, Johnson JK, Yano BL, Perry R, Schafer K, Society of Toxicologic Pathology position paper: organ weight recommendations for toxicology studies, Toxicol Pathol, 35 (2007) 751–755. [PubMed: 17849358]

[57]. Rauchhaus U, Schwaiger FW, Panzner S, Separating therapeutic efficacy from glucocorticoid side-effects in rodent arthritis using novel, liposomal delivery of dexamethasone phosphate: long-term suppression of arthritis facilitates interval treatment, Arthritis Res Ther, 11 (2009) R190. [PubMed: 20003498]

[58]. Chiang JL, Patterson R, McGillen JJ, Phair JP, Roberts M, Harris K, Riesing KS, Long-term corticosteroid effect on lymphocyte and polymorphonuclear cell function in asthmatics, J Allergy Clin Immunol, 65 (1980) 263–268. [PubMed: 7358943]

Author Manuscript Author Manuscript Author Manuscript Author Manuscript

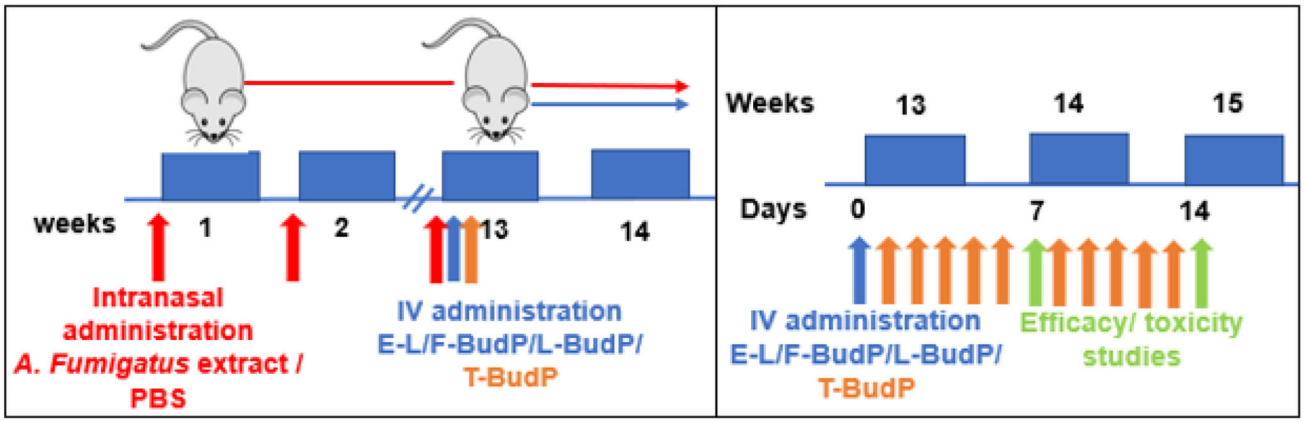

Fig. 1.

Study design to determine the efficacy and toxicity of intravenously administered L-BudP treatment in a mouse model of *A. fumigatus* extract-induced CRS over a 14-week study period. Blue boxes represent weeks. Chronic rhinosinusitis (CRS), empty liposomes (E-L), free budesonide phosphate (F-BudP), liposomal budesonide phosphate (L-BudP), topical budesonide phosphate (T-BudP), intravenous (IV), *A. fumigatus* (*Aspergillus fumigatus*).

Author Manuscript Author Manuscript Author Manuscript Author Manuscript

A

	L-BudP	E-L
	Mol %	Mol %
HSPC	58.0	58.0
Cholesterol	37.0	37.0
DSPE-PEG2000	5.0	5.0
Size (diameter) (nm)	153.5 ± 4.1	150.9 ± 2.7
PDI	0.12 ± 0.02	0.12 ± 0.01
Zeta potential (mV)	-14.6 ± 2.3	-14.1 ± 3.5
BudP (mg/ml)	3.78 ± 0.65	NA

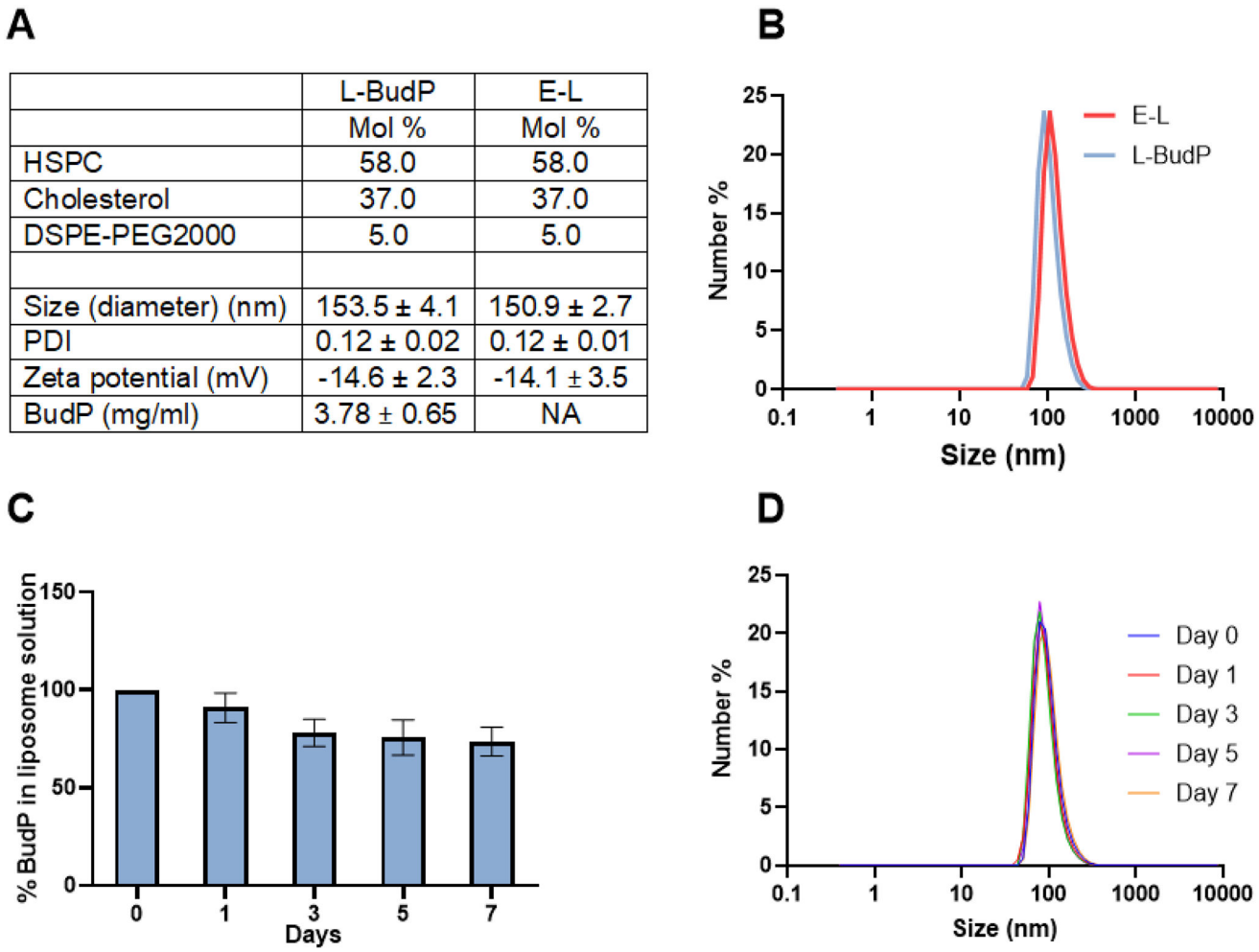

Fig. 2.

Synthesis and characterization of liposomes. A) Characteristics of synthesized liposomes (theoretical mole % of lipids; Size, PDI, and zeta potential of liposomal batch measured using DLS), B) size distribution spectrum, C) release study in SBF; % BudP present in liposomes measured with high-performance liquid chromatography (HPLC), D) colloidal stability of L-BudP in SBF in terms of size measured with DLS. Liposomal batches were assessed in triplicate, and the data are represented as the mean ± SD. Budesonide phosphate (Bud-P), empty liposomes (E-L), liposomal budesonide phosphate (L-BudP).

Author Manuscript Author Manuscript Author Manuscript Author Manuscript

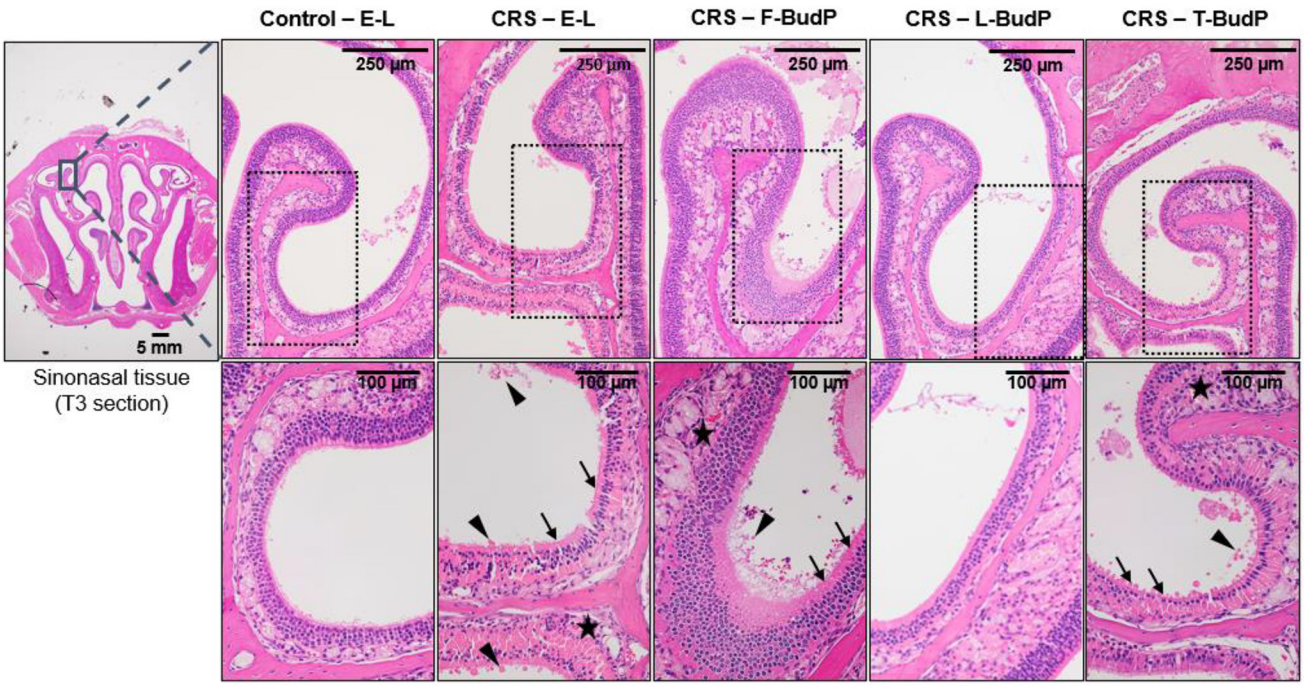

Fig. 3.

L-BudP treatment reduced CRS-associated sinonasal inflammation, as assessed through histopathological examination of H&E-stained tissues. CRS mice showed degenerative changes to the epithelial cell barrier (arrow) with apical blebbing (arrowhead), goblet cell hyperplasia, thickening of basement membrane, and infiltration of immune cells in the subepithelial region (star). L-BudP treatment resulted in marked tissue remission compared to F-BudP and T-BudP treatment. The coronal section of sinonasal tissue (T3 section) shown at the left. The top row shows higher magnification of ethmoid turbinate from different treatment groups. The bottom row shows higher magnification of regions (dotted box) indicated in ethmoid turbinate. Chronic rhinosinusitis (CRS), empty liposomes (E-L), free budesonide phosphate (F-BudP), liposomal budesonide phosphate (L-BudP), topical budesonide phosphate (T-BudP).

Author Manuscript Author Manuscript Author Manuscript Author Manuscript

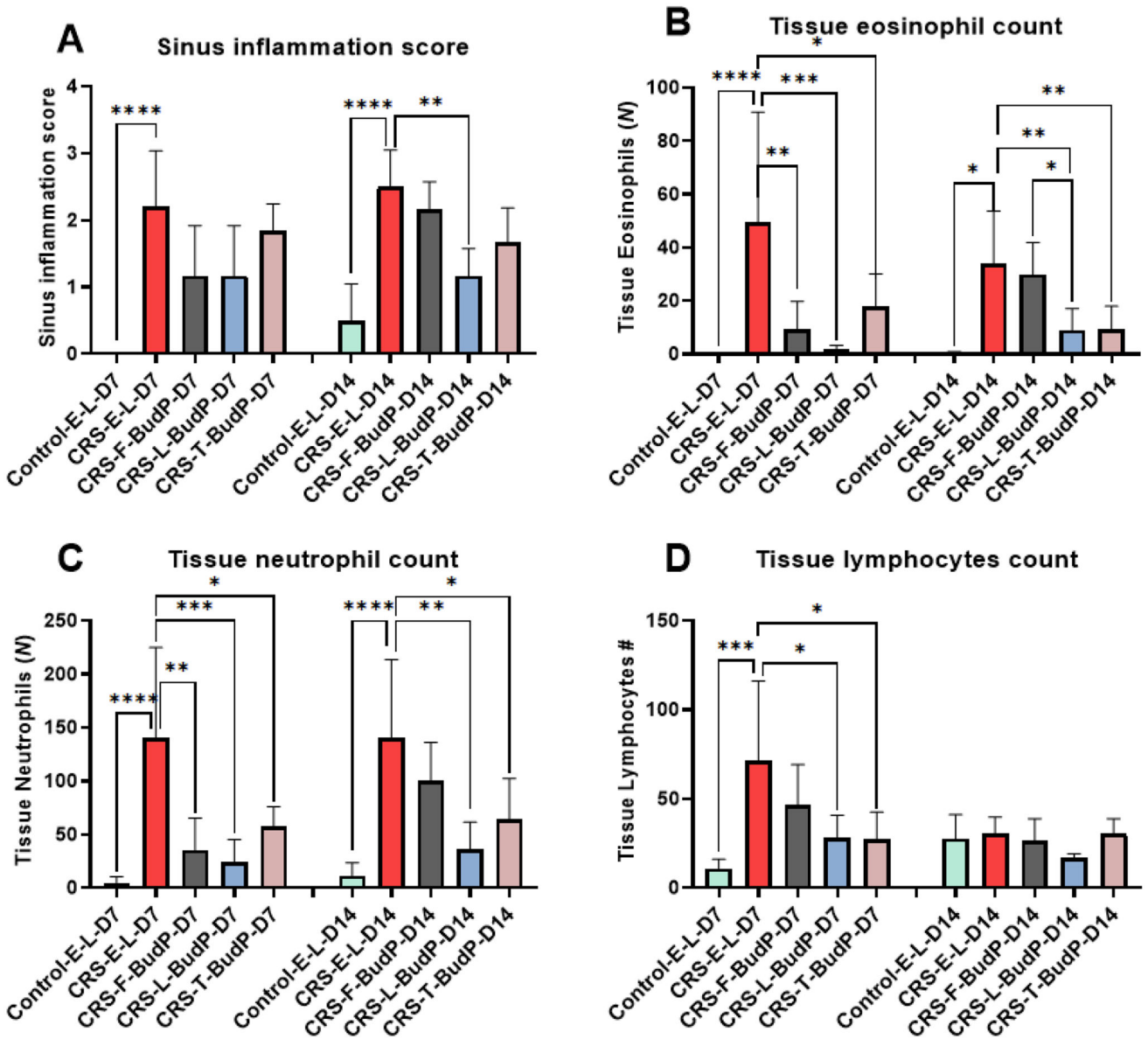

Fig. 4.

L-BudP treatment significantly reduced CRS-associated sinonasal inflammation and immune cell infiltration into the sinonasal tissue (n ≥ 5). A) Overall inflammation scores determined through pathological examination at days 7 and 14 after tail vein injection in CRS mice. Pathological enumeration of B) eosinophils, C) neutrophils, and D) lymphocytes at days 7 and 14 after tail vein injection in CRS mice. Data are represented as the mean ± SD. (*p< 0.05; **p< 0.01; ***p< 0.001; ****p< 0.0001). Chronic rhinosinusitis (CRS), empty liposomes (E-L), free budesonide phosphate (F-BudP), liposomal budesonide phosphate (L-BudP), topical budesonide phosphate (T-BudP).

Author Manuscript Author Manuscript Author Manuscript Author Manuscript

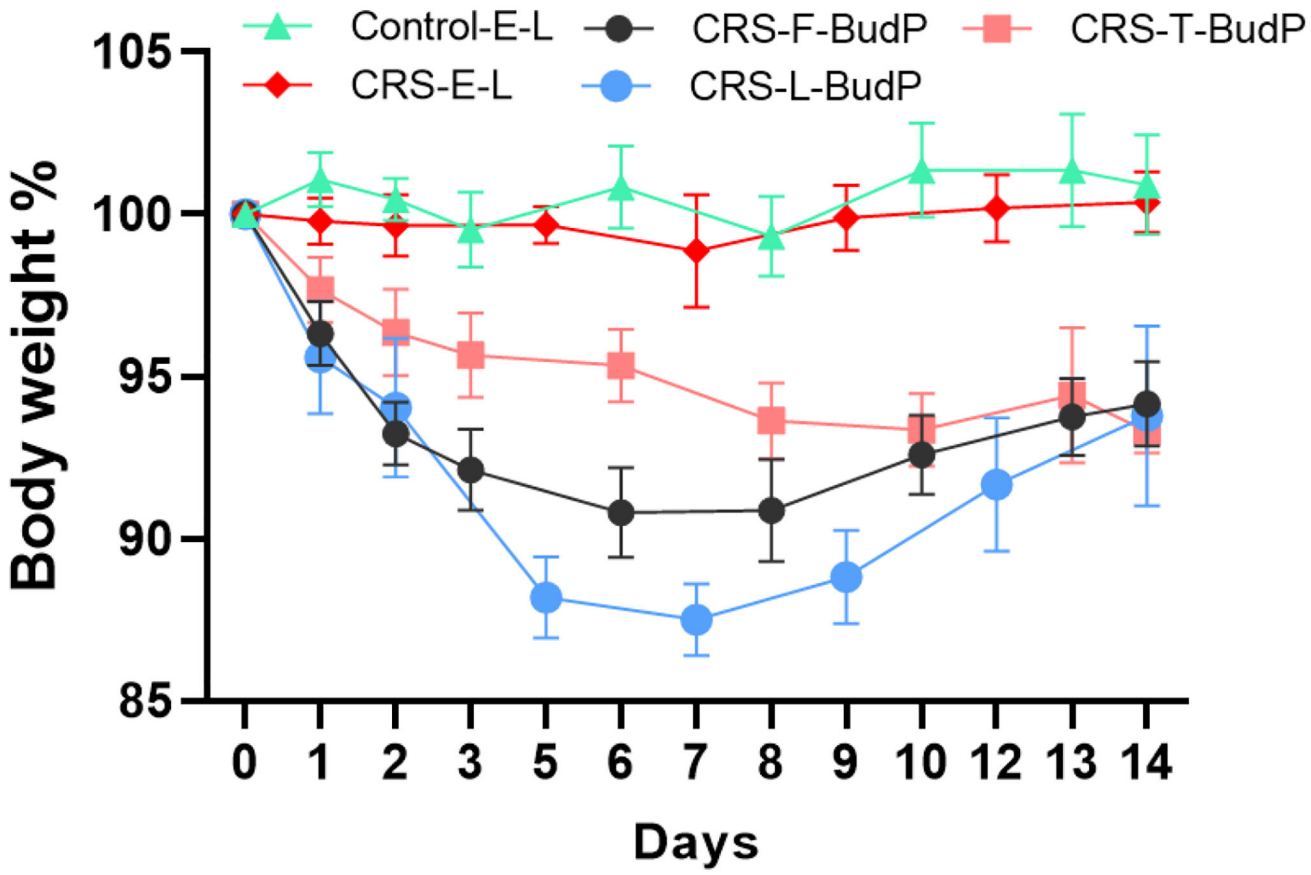

Fig. 5.

Effect on total body weight % due to different treatments. BudP treatment transiently affected animal body weights ($n \geq 5$). E-L treatment did not affect body weight. Data are represented as the % mean from initial body weight ± SD. Chronic rhinosinusitis (CRS), empty liposomes (E-L), free budesonide phosphate (F-BudP), liposomal budesonide phosphate (L-BudP), and topical budesonide phosphate (T-BudP).

Author Manuscript Author Manuscript Author Manuscript Author Manuscript

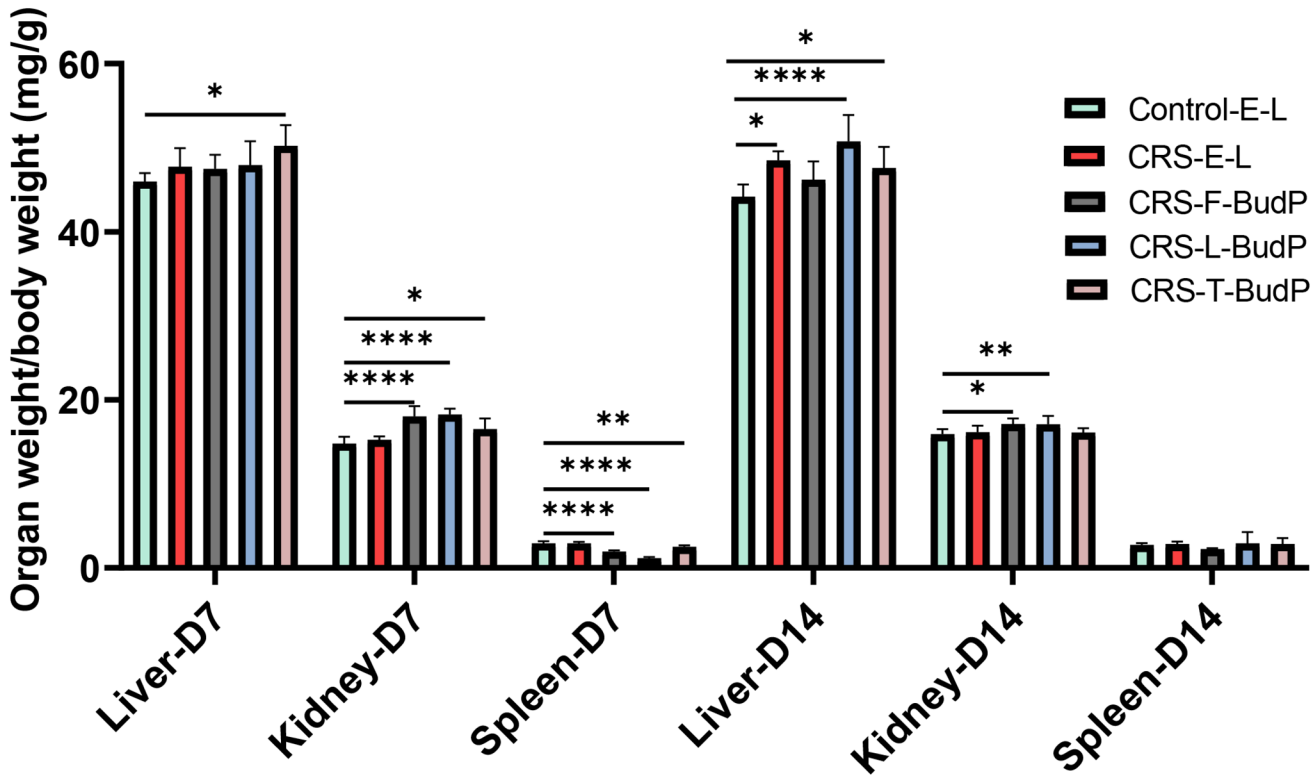

Fig. 6.

Effect on organ weight-to-body weight ratio due to different treatments at day 7 and day 14 (n ≥ 5). Data are represented as the mean ± SD. (*p<0.05, **p<0.01, ***p<0.001, ****p<0.0001). Chronic rhinosinusitis (CRS), empty liposomes (E-L), free budesonide phosphate (F-BudP), liposomal budesonide phosphate (L-BudP), and topical budesonide phosphate (T-BudP). Data are represented as the mean ± SD.

Author Manuscript Author Manuscript Author Manuscript Author Manuscript

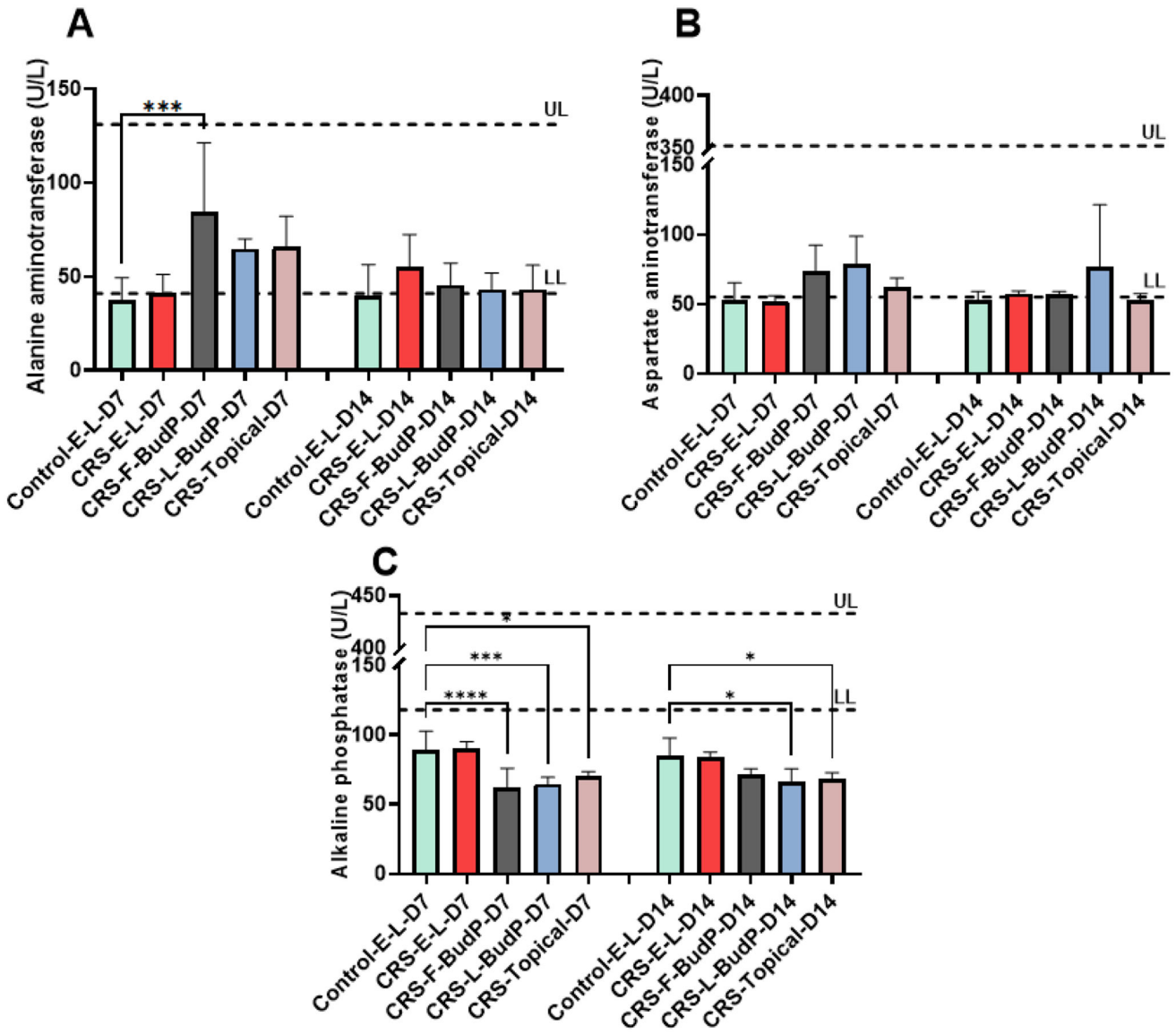

Fig. 7.

The effect of BudP on blood liver enzyme levels, assessed at day 7 and day 14 after tail vein injection (n ≥ 5). ALT and AST enzymes at day 7 and day 14 were within normal range across all treatment groups. Peripheral blood levels of A) ALT (U/L), B) AST (U/L), and C) AP (U/L). N ≥ 5, Data are represented as the mean ± SD. (*p<0.05, **p<0.01, ***p<0.001, ****p<0.0001, NS not significant). Chronic rhinosinusitis (CRS), empty liposomes (E-L), free budesonide phosphate (F-BudP), liposomal budesonide phosphate (L-BudP), topical budesonide phosphate (T-BudP), Alanine aminotransferase (ALT), aspartate aminotransferase (AST), and alkaline phosphatase (AP), Upper Limit (UL), Lowe Limit (LL).

Author Manuscript Author Manuscript Author Manuscript Author Manuscript

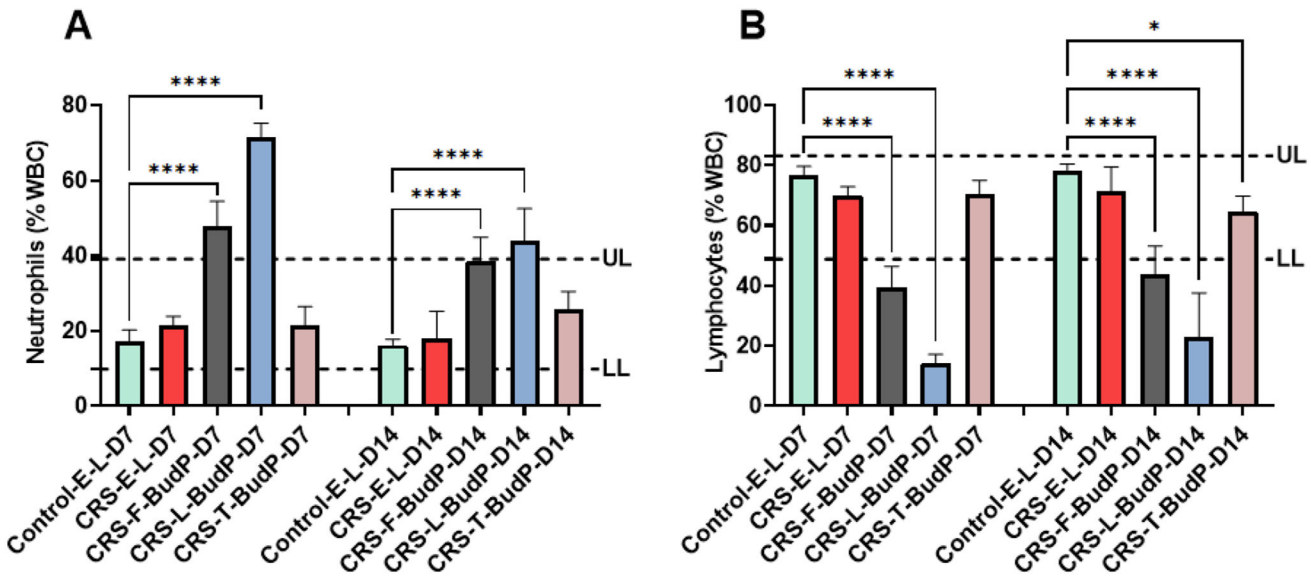

Fig. 8.

BudP treatment transiently affected the peripheral blood immune cell counts, assessed at days 7 and 14 after tail vein injection (n ≥ 5). Differential cell analysis for: A) lymphocytes, and B) neutrophils for all groups. N ≥ 5, Data is represented as the % mean of white blood cells ± SD (*p<0.05, **p<0.01, ***p<0.001, ****p<0.0001). Chronic rhinosinusitis (CRS), empty liposomes (E-L), free budesonide phosphate (F-BudP), liposomal budesonide phosphate (L-BudP), and topical budesonide phosphate (T-BudP). Upper Limit (UL), Lower Limit (LL), White Blood Cells (WBC).

Author Manuscript

Author Manuscript

Author Manuscript

Author Manuscript

Table 1.

Treatment groups and timepoints for the animal study.

	Treatment	BudP Concentration	Day 7	Day 14
			Mice #	Mice #
Control	E-L	NA	6	6
CRS	E-L	NA	5	6
	F-BudP	10 mg/kg	6	6
	L-BudP	10 mg/kg	6	6
	T–BudP	5 μg/nostril/dose/day	6	6

Chronic rhinosinusitis (CRS), empty liposomes (E-L), free budesonide phosphate (F-BudP), liposomal budesonide phosphate (L-BudP), topical budesonide phosphate (T-BudP).